UNCLASSIFIED

Defense Technical Information Center
Compilation Part Notice

ADP014283

TITLE: Nanomechanical Characterization on Zinc and Tin Oxides Nanobelts

DISTRIBUTION: Approved for public release, distribution unlimited

This paper is part of the following report:

TITLE: Materials Research Society Symposium Proceedings Volume 740 Held in Boston, Massachusetts on December 2-6, 2002. Nanomaterials for Structural Applications

To order the complete compilation report, use: ADA417952

The component part is provided here to allow users access to individually authored sections of proceedings, annals, symposia, etc. However, the component should be considered within the context of the overall compilation report and not as a stand-alone technical report.

The following component part numbers comprise the compilation report:
ADP014237 thru ADP014305

UNCLASSIFIED

Mat. Res. Soc. Symp. Proc. Vol. 740 © 2003 Materials Research Society I9.5

Nanomechanical Characterization on Zinc and Tin Oxides Nanobelts

Minhua Zhao[1] Scott Mao[1], Zhong Lin Wang[2] Fengting Xu[3] and John A Barnard[3]
[1] Department of Mechanical Engineering, Univ. of Pittsburgh, Pittsburgh, PA 15261
[2] School of Materials Sci. & Engr. , George Institute of Technology, Atlanta, GA 30332-0245
[3] Department of Materials Sci. & Engr., Univ. of Pittsburgh, Pittsburgh, PA 15261

ABSTRACT

Nanobelts are a group of materials that have a rectangle-like cross section with typical widths of several hundred nanometers, width-to-thickness ratios of 5 to 10, and lengths of hundreds of micron meters. In this paper, nanoindentations were made on individual ZnO, SnO_2 nanobelts and (0001) bulk ZnO by using AFM and Hysitron Triboscope indenters. It was shown that the indentation size effect was still obvious for the indentation depth under 50 nm. It is also demonstrated that nanomaching is possible on nanobelt using AFM tip.

INTRODUCTION

In recent years, quasi one-dimensional (1D) solid nanostructure (nanowires and nanobelts) have stimulated considerable interest for scientific research due to their importance in mesoscopic physics studies and their potential applications. Compared to micrometer diameter whiskers and fibers, these nanostructures are expected to have remarkable optical, electrical, magnetic, and mechanical properties. Exploration of novel methods for large-scale synthesis of 1D nanostructure is a challenging research area. As n-type semiconductive materials, zinc oxide (ZnO) has received a considerable amount of attention over last few years because of many applications it has found in various fields. ZnO is now widely used as transparent conducting oxide materials and gas sensors. In particular, ZnO is regarded as a promising candidate material for flat panel displays because of its high electrical conductivity, high optical transparency as well as its low cost and easy etchability.

Recently, Wang's group [1-3] has successfully synthesized the belt-like oxides (so called nanobelts) by evaporating ZnO or SnO_2 powders at high temperatures without the presence of catalyst. The beltlike morphology is distinct from those of semiconductor nanowires. With a well-defined geometry and perfect crystallinity, the semiconducting oxide belts are likely to be a model materials family for understanding mechanical behavior at nano-scale with absence of dislocations and defects (excluding point defects). The dimension of the nanobelt as a mechanical cantilever potentially can be used as a mechanical resonator, or as electro-optical resonator. Due to its small dimension, the natural frequency (resonance) of the nanobelt, as a resonator could be very high. Since the nanobelt can be used as nanomechanical device, it is important to measure its elastic Young's modulus and strength as well as fracture stress. The nanobelts provide an ideal object for characterizing the mechanical behavior of defect-free semiconducting oxides at nano-scale. In this study, nano-scale mechanical properties of individual zinc oxide nanobelts were characterized by Nanoscope IIIa AFM and Hysitron TriboScope with homemade side view CCD camera. It was shown that the indentation size effect was still obvious for the indentation depth under 50 nm. It is also demonstrated that nanomaching is possible on nanobelt using AFM tip.

EXPERIMENTAL DETAILS

The synthesis of nanobelts was based on thermal evaporation of oxide powders under controlled conditions without presence of catalyst [1-3]. The procedures of preparing dispersed nanobelts for the study reported here are as follows [4]: first immerse the wool like nanobelts in acetone, and the mixture was dispersed by ultrasonic cleaning device. Then dip the polished silicon wafer into the solution and pull out. After drying, single nanobelt lying on silicon substrate.

The prepared nanobelt sample was investigated by two means: one is by tapping mode of Nanoscope IIIa, using diamond indenter tip with a radius of < 25 nm. The other is by STM mode of Hysitron TriboScope, an add-on force transducer from Hysitron Inc., using diamond cubic corner tip with a radius of < 40 nm. In either case, individual nanobelts were imaged, and then nanoindentations were made on the nanobelt using varied loads. After indentation, the indent was imaged in-situ using the image mode of the AFM. For nanoindentations, the hardness is normally defined as the maximum load divided by the projected area of the indenter in contact with the sample at the maximum load. Thus,

$$H = \frac{P_{MAX}}{A_C} \tag{1}$$

where H, P_{MAX} and A_C are hardness, maximum applied load and projected contact area at the maximum applied load, respectively. Since the indenter tip is not rigid during indentation, the elastic modulus can not be directly determined from the load versus displacement curve. However, the reduced elastic modulus can be determined from the unloading portion of the curve by the relation:

$$E_r = \frac{\sqrt{\pi}}{2} \cdot \frac{dP}{dh} \cdot \frac{1}{\sqrt{A_c}} \tag{2}$$

where Er and dP/dh are reduced modulus and experimentally measured stiffness, respectively.

DISCUSSIONS

Figure 1a is a three dimensional image of ZnO nanobelt before indentation. Section analysis shows the nanobelt has a rectangular section. The width of the nanobelt is about 360 nm and the height is about 65 nm. This gives a width-to-thickness ratio of 5.5. These values are typical of a single nanobelt. More investigations using transmission electron microscopy reveal that nanobelt have a rectanglelike cross section with typical widths of several hundred nanometers, width-to-thickness ratios of 5 to 10, and lengths of hundreds of micron meters by TEM. Because the material was already an oxide, it did not undergo a chemical reaction, and had a pure, flawless surface. More importantly, each belt is single crystalline without dislocation. Flawlessness is a major advantage since flaws between crystals can cause problems such as heat generated by flaws when current flows, which is important for nano-scale electronics to increase the density of devices.

After zinc oxide single nanobelt was lying on silicon substrate, the nanobelt was indented by a nanoindentor under AFM. The applied load was recorded as function of penetration. After the nanoindentation, AFM imaging was taken to study local mechanical behavior. Figure 1b is a local magnification of nanoindentations on the nanobelt, where 3 triangle nanoindentations can be found. Figure 2a shows the typical load vs. deflection curves for ZnO and SnO_2 nanobelts on

their top surfaces, which are $(2\bar{1}\,\bar{1}\,0)$ and $(10\bar{1})$, respectively. From the slope of the loading curves, we can find that the SnO_2 nanobelt is stiffer than ZnO nanobelt. Based on Equation (1), using load vs. deflection curves during nanoindentation, hardness of ZnO and SnO_2 nanobelts was calculated as function of indentation penetration, and the result is summarized in Fig. 2b. The hardness of ZnO is lower than that in SnO2 nanobelt. Also it can be seen that the lower penetration of the nanoindentation, the higher the hardness of the nanobelt, which is attributed to the strain gradient effect (size effect) during nanoindentation for most materials [5-6].

Comparison of ZnO nanobelt with ZnO bulk single crystal was carried out on (0001) plane by nanoindentation. As shown in Fig 3, ZnO nanobelt is little softer than that of bulk single crystal. This is likely due to that the (0001) is the most close packed plane for hexagonal structured ZnO, thus, the hardness along [0001] (the c-axis) may be higher than that along $[2\bar{1}\,\bar{1}\,0]$ (the a-axis), which is the normal direction of the nanobelt.

Based on Equation (2), from load vs. deflection curves, elastic modulus of ZnO and SnO_2 nanobelts are calculated as a function of the indentation penetration. As shown in Fig. 4, the elastic modulus of the SnO_2 is higher than that of ZnO. The increase of elastic modulus leads to the increase of the hardness for SnO_2 nanobelt compared to that of the ZnO nanobelt, which was given in Figure 2b.

Nano-indentation induced fracture test on SnO_2 also was carried out by increasing a large indentation loads on the nanobelt. Figure 5a shows a crack induced by nano-indenation, which was initiated from a triangle edge on the indentation. The crack propagates along [101], and the cleavage surface is (010) based on the structural information provided by electron microscopy [1]. Figure 5b is the indentation load vs. penetration curve, which indicates unstable crack propagation when 43 micro-Newton of indentation load is applied. This is probably the load at which the crack is created. After the penetration reaches 60 nm (~ belt thickness), nanoindentor starts indenting Si substrate and the load starts picking-up since Si substrate is harder than SnO_2 crystal. The fracture test on SnO_2 demonstrated the possibility to cut or machine the nanobelt under AFM down to smaller size.

CONCLUSIONS

Imaging, manipulating and testing on mechanical properties of a single nanobelt of ZnO and SnO_2, whose size is in the nano- to micron-meter range, have been performed using atomic force microscope. The hardness and elastic modulus of the ZnO nanobelt is smaller than that of SnO_2. Furthermore, the hardness of dislocation free ZnO nanobelt is slightly smaller than that of the c-axis oriented bulk ZnO single crystal, which may be attributed to the anisotropic structure of the ZnO.

ACKNOWLEDGEMENTS

The authors are grateful to the support from NSF Grant No. CMS-0140317 to University of Pittsburgh and NSF Grant No. DMR-9733160 to Georgia Tech.

REFERENCE

1. Zheng Wei Pan, Zurong Dai and Zhong Lin Wang et al, Nanobelts of Semiconducting Oxides, Science, 9 March 2001, pp. 1947-9.
2. Z.R. Dai, Z.W. Pan and Z.L. Wang, Solid State communications 118 (2001), 351-354.
3. Z.W. Pan, Z.R. Dai and Z.L. Wang, Applied Physics Letters, Vol. 80 No.2, January 2002, P. 309
4. Scott Mao, M. Zhao, and Zhong Lin Wang, MRS 2002 fall Symposium F: Semiconductor Materials and Devices, Boston Dec. 2-6, 2002.
5. D. M. Duan, N. Wu, W.S. Slaughter, S.X. Mao, *Mat. Sci. & Eng. A. A303 (2001) 241-249.*
6. B. M. Ennis, W. Slaughter, Anita Madan and S.X. Mao, submitted to Acta Materialia.

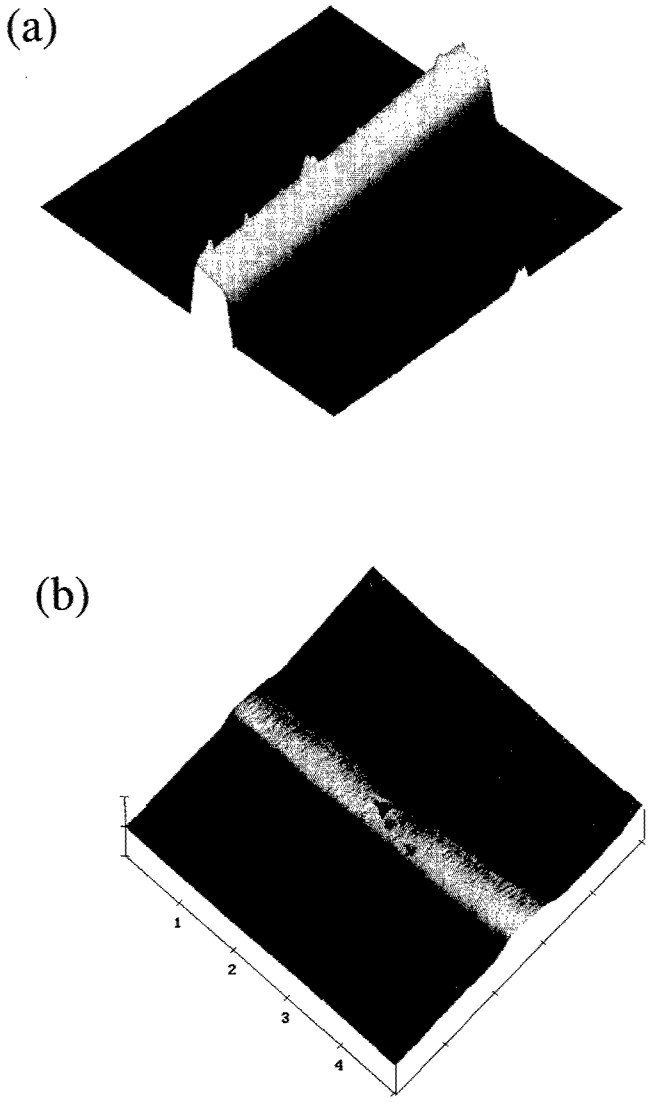

Figure 1. (a) Three dimensional image of ZnO nanobelt imaged by AFM indenter tip; (b) Indentation on ZnO nanobelt by AFM indenter.

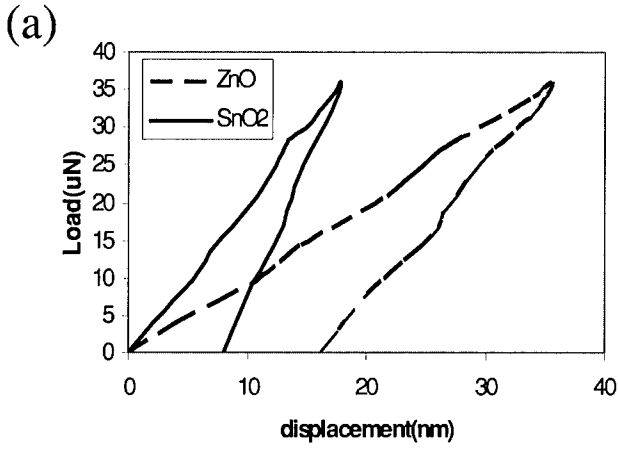

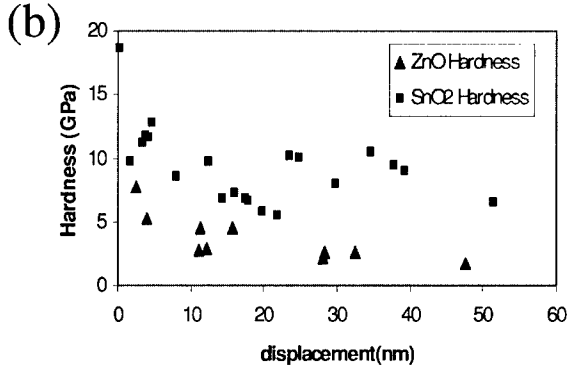

Figure 2. (a) Load vs. deflection curve during nanoindentation under AFM. The stiffness of SnO_2 is larger than that of ZnO nanobelt. (b) Hardness of ZnO and SnO_2 nanobelts as function of penetration during nanoindetation.

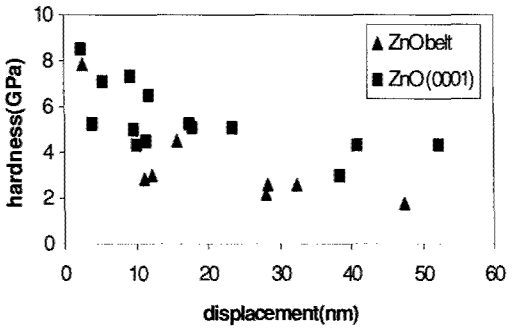

Figure 3. Hardness for ZnO nanobelt and bulk single crystal (0001).

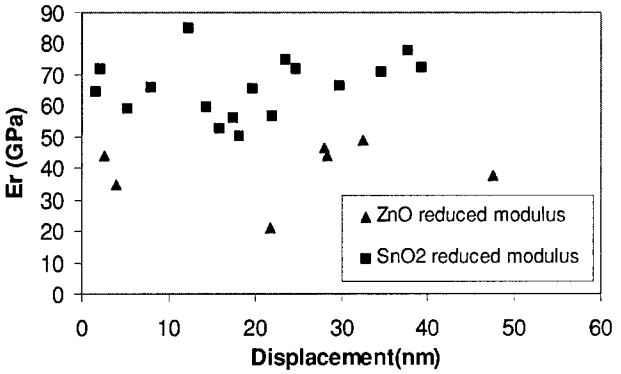

Figure 4. Elastic modulus of ZnO and SnO_2 nanobelts as function of penetration during nanoindetation

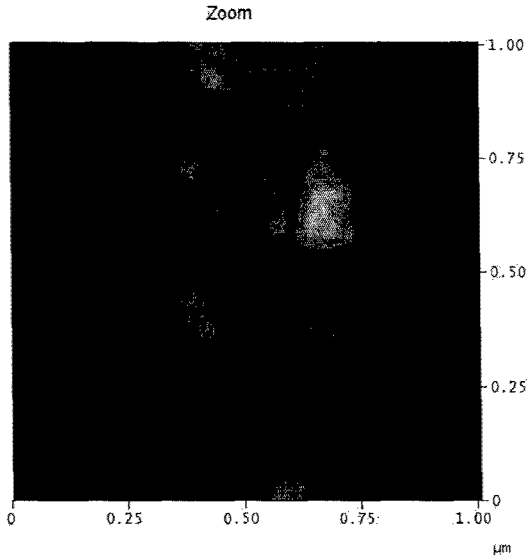

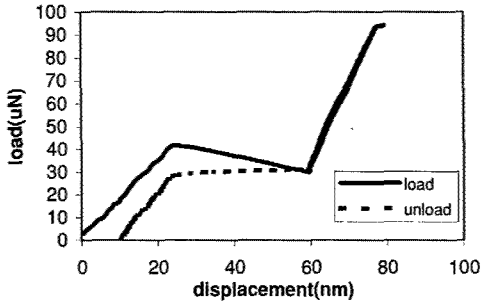

Figure 5. Crack nucleation and propagation in SnO_2 nanobelt by nanoindentation under AFM, (a) a crack induced by nano-indenation and (b) indentation load vs. penetration curve, which indicates unstable crack propagation when 43 micro-Newton of indentation load is applied.